RICE UNIVERSITY

New Metrics on Image Articulation Manifolds Using Optical Flow

by

Sriram Nagaraj

A THESIS SUBMITTED
IN PARTIAL FULFILLMENT OF THE
REQUIREMENTS FOR THE DEGREE

Master of Science

APPROVED, THESIS COMMITTEE:

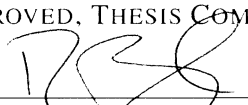

Richard G. Baraniuk, Chair,
Victor E. Cameron Professor,
Electrical and Computer Engineering

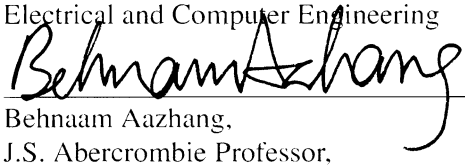

Behnaam Aazhang,
J.S. Abercrombie Professor,
Electrical and Computer Engineering,
ECE Department Chair

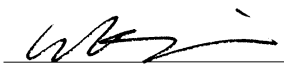

Wotao Yin,
Assistant Professor,
Computational and Applied Mathematics

HOUSTON, TEXAS

APRIL 2011

Abstract

New Metrics on Image Articulation Manifolds Using Optical Flow

Image articulation manifolds (IAMs) arise in a wide variety of contexts in image processing and computer vision applications. IAMs are a natural nonlinear model for image ensembles generated by the variation of imaging parameters (scale, pose, lighting etc.). In the past, IAMs have been studied as being embedded submanifolds of higher dimensional Euclidean spaces. However, this view suffers from two major defects: lack of a meaningful metric and reliance on linear transport operators via tangent vectors. Recent work in the area indicates the existence of better *nonlinear* transport operators for IAMs, with optical flow based transport being a prime candidate. In this thesis, we provide a detailed theoretical analysis of optical flow based transport on IAMs. In particular, we develop new *analytical* tools reminiscent of differential geometry to handle the apriori *data driven* nature of IAMs using the notion of *optical flow manifolds (OFMs)*. We define an appropriate metric on the IAM via a metric on the corresponding OFMs that satisfy certain local isometry conditions and we show how to use this new metric to develop a host of mathematical tools such as optical flow fields on the IAM, parallel fields and parallel transport as well as an intuitive notion of "optical curvature". We show that the space of optical flow fields along a path of constant optical curvature has a natural multiscale structure. We also consider the question of approximating non-parallel flow fields by parallel flow fields.

Acknowledgements

I first thank both Sri Kanchi Kamakshi and Sri Akhilandeshwari for being the inspiration and enlivening forces in me. I thank my parents, Sri Nagaraj Venkat and Smt. Hemalatha Nagaraj for their constant encouragement, support and complete belief in me. I also thank my uncle, Dr. Narayanan Ramamamurthy for his sincere encouragement and frank opinions on life in general.

I owe an unpayable debt of gratitude to my one-of-a kind advisor, Dr. Richard Baraniuk. More than anything, his kind words during a certain rough patch of my studies went a long way in giving me confidence and enthusiasm. He has shown by example that life in academics is not divorced from fun and merriment, and that being a kind, sincere and considerate human being is as important as good research. Thank you Rich! Special thanks to Dr. Behnaam Aazhang and Dr. Wotao Yin for their useful comments that improved the quality of this work.

The work in this thesis would not be possible without the help, insight and encouragement of Aswin Sankaranarayanan. Thanks also to Chinmay Hegde, Eva Dyer and Arian Maleki (to whom I owe a proof sketch) for their feedback. I gratefully acknowledge their help. Last, but certainly not the least, I greatly thank Sri Narayan Dave and family, Sri Jeevanji and family, Sri Gopal Salvady and the rest of the Namadwaara family for many divine weekends.

Dedication

This thesis is humbly dedicated to my parents. *Namo Namah Sri Guru Padukabhyam*

Contents

List of Figures

Chapter 1

Introduction

Many problems in image processing and computer vision involve ensembles of images from which one extracts relevant information for analysis and processing. Often, the image ensembles are generated by varying a set of imaging parameters such as pose, lighting, viewing angle etc. of a fixed three dimensional object or scene. As the imaging parameters vary, the space of images thus formed is known to form a typically nonlinear manifold called an *image articulation manifold (IAM)* [9, 29]. Each point on an IAM is an image at a particular parameter value. For instance, a typical IAM used for face recognition applications would consist of images of a human face undergoing changes in lighting and/or orientation. The manifold model naturally accounts for nonlinearities in the image ensembles and provides a powerful framework for processing parametric families of images.

Understanding the structure of IAMs is an important and difficult problem as the geometric structure of the IAM depends on both the scene as well as the imaging parameters. Image processing algorithms on IAMs must therefore be able to identify and utilize the inherent structure of the IAM for a variety of tasks such as recognition, classification, clustering etc.

1.1 Stylized Applications of IAMs

As the structure of an IAM reflects the changes in the scene, inferring the geometry of the IAM and understanding its relationship with the scene and imaging parameters has profound implications for applications. Specifically, we list the following stylized examples.

- *Image interpolation and manifold navigation*: Given two images (points) on an IAM, consider the task of transforming one image into another such that the intermediate points also lie on the IAM, i.e., the task is to generate a path on the IAM between the two images. A related task is manifold navigation, i.e., given a template image on the IAM, we would like to navigate from the template image to other images in a neighborhood of the template image. As we shall see, traditional linear approaches using *linear transport* on the manifold via tangent spaces are extremely limited in their ability to interpolate between the two images. This motivates the search for more effective *nonlinear* methods.

- *Video processing*: A video $\mathcal{I}$ is a sequence of time indexed images $\{I_n, n = 0, 1, \cdots, N\}$ for some integer $N > 0$, or more generally in the continuous case, $\mathcal{I} = \{I_t, 0 \leq t \leq T\}$ for some $T > 0$. From the continuous viewpoint, we can thus regard a video as a parametric curve on an IAM. Classical applications such as video coding, motion compensation and compression now can be reformulated from the manifold standpoint, and understanding the structure of the IAM will pave the way for efficient video processing algorithms.

- *Parameter Estimation*: Given an image I on an IAM M, consider the task of recovering the corresponding parameter $\theta \in \Theta$ such that $i(\theta) = I$. As the IAM consists of parametric images, an optimal estimate for the parameter θ can be used for efficient recognition/classification tasks on the IAM.

There are numerous other applications in imaging processing involving manifolds: for instance, homogeneous manifolds have been used in [1] for efficient detection and estimation via representations of compact Lie groups. By considering a family or collection of different IAMs generated by the *same* set of parameters, we can use the joint information of the family for data fusion [7]. This use of multiple information sources has great advantages while dealing with military and reconnaissance applications.

1.2 Challenges with IAMs

Considering an image I as a square integrable function $[0,1]\times[0.1] \to \mathbb{R}$ leads to IAMs being viewed as submanifolds of $L^2([0,1] \times [0,1])$. This view, though helpful, has certain disadvantages. First, as shown in [9, 29], IAMs are plagued by *non-differentiability* issues. Specifically, using the L^2 metric as the distance between images, it follows that the distance $\|I_1 - I_2\|_{L^2}$ between images I_1 and I_2 is a non-differentiable function $\eta(\|\theta_1 - \theta_2\|)$ of the corresponding parameter values θ_1, θ_2 that is asymptotically equivalent to $(\|\theta_1 - \theta_2\|)^{\frac{1}{2}}$. Indeed, $\frac{\|I_1 - I_2\|_{L^2}}{\|\theta_1 - \theta_2\|} \geq c\|\theta_1 - \theta_2\|^{-\frac{1}{2}}$ so that for images with sharp edges, the corresponding IAM is non-differentiable. Moreover, as intrinsic geodesics have infinite length under embedding via the L^2 metric, the authors in [9] are forced to define a "normalized geodesic

distance" and carry out further analysis. To alleviate the non-differentiability problem, [29] resort to a multiscale smoothing procedure that involves regularizing each point of the IAM by a Gaussian smoothing filter at different scales which renders the IAM smooth across the various scales. This smoothing procedure then allows for the definition of tangent spaces on which one can perform standard linear methods of analysis.

However, the fundamental problem associated with the above line of approach is the lack of a metric that reflects the parameter changes. Consider for example the IAM generated by imaging a black disk of radius R translating on an infinite white background using the L^2 metric $\|I_1 - I_2\|_{L^2}$ between images. Let I_1 be the image of the disk with center c_1 and I_2 the image of the disk with center c_2. It then follows that $\|I_1 - I_2\|_{L^2}$ is:

$$\begin{cases} \eta(\|c_1 - c_2\|), & \|c_1 - c_2\| < 2R \\ D, & \|c_1 - c_2\| \geq 2R \end{cases} \tag{1.1}$$

where D is a constant that depends on the radius R of the disk. Thus, when the disk centers are separated by a distance greater than $2R$, the metric is completely uninformative: additional changes in parameters do not affect the measured distance.

Finally, differential geometric tools are rarely used for IAMs, even after appropriate smoothing. This is due to the fact that IAMs typically lack *analytic* structure by which we mean we do not have analytic expressions for geodesics, affine connections etc. on IAMs. In the absence of analytic tools, algorithms for IAMs involve computational techniques such as ISOMAP [25], Locally Linear Embedding (LLE) [20], Laplacian LLE [2]

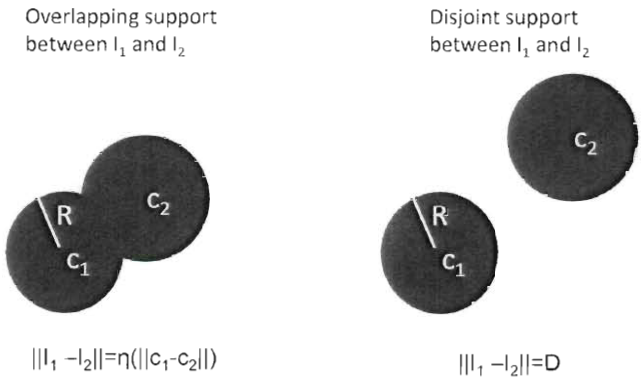

Figure 1.1: The IAM generated by imaging a translating disk on an infinite white background. Here, the L^2 distance between two images of the disk with centers c_0 and c_1 is a nonlinear function $\eta(c_0, c_1)$ when the separation between the centers is less than $2R$. When the disk separation is greater than $2R$, the distance is a constant D and further changes in parameter values do not effect any change in the distance.

etc. However, these methods have two main limitations. First, they are *linear* methods that locally approximate the manifold using tangent spaces and perform principal component analysis or other related eigen-analysis while ignoring the often critical curvature properties of the IAM. Moreover, these methods are extrinsic, i.e., depend on particular embeddings of the IAM in Euclidean space. Second, these methods are applied to arbitrary data modeled as having manifold structure, and are not specific to the case of IAMs (for instance, probabilistic methods such as diffusion geometry ([5, 17]) have a "point cloud" view of data) which, as we have seen, come with more structure than generic data.

1.2.1 Example: Image interpolation:

Consider the example of image interpolation. While linear motion along tangent vectors provides infinitesimal transport, it is not possible to use linear motion while staying on the

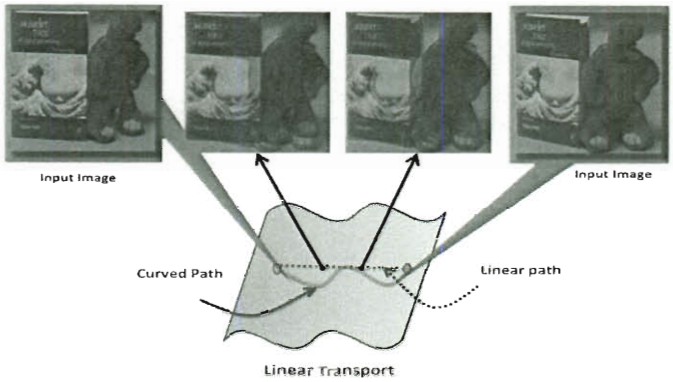

Figure 1.2: Linear transport on IAMs. Linear methods do not provide extensive transport on the IAM as is evident from the blurred intermediate images between the two input images.

manifold for extended distances. Linear motion between two images I_1, I_2 accounts for the convex combination $\alpha I_1 + (1 - \alpha) I_2$ of I_1 and I_2 $(0 \leq \alpha \leq 1)$, while generic IAMs are *not* affine and hence linear transport results in intermediate images that lie outside the IAM of interest, showing that linear transport is valid only locally. As a concrete example, consider image interpolation as shown in Fig. 1.2. Here, we would like to find a path between the two input images which respects the manifold geometry. However, linear transport obtained by linear interpolation in the direction of the tangent vector between the two images results in blurring which shows that the intermediate images do not lie on the IAM, i.e., linear methods fail to transport the base image along the manifold for significant distances.

In summary, previous approaches to IAM analysis are limited by both lack of analytic tools as well as methods that take curvature of the IAM into consideration. It is clear that the linearity constraint as well as lack of analytic tools do not allow us to realize the goal of processing IAMs using their inherent geometry and severely restrict the possibility of

novel applications. The tools developed in this thesis will help to bridge this gap and pave the way for analytic methods in IAM analysis. As we shall see, the tools we develop rely on an appropriate metric on the IAM using nonlinear *transport operators*.

1.3 Transport Operators

An emerging paradigm in handling the linear approximation constraint mentioned above is the notion of *transport operators* [21]. Roughly, a transport operator on an IAM is a (often nonlinear) map from the manifold into itself that allows one to move between different points on the manifold. Given images $I_0(\mathbf{x})$ and $I_1(\mathbf{x})$, (where $I(\mathbf{x})$ denotes the intensity at the spatial location $\mathbf{x} = (x, y) \in [0, 1] \times [0, 1]$) a transport operator T ia a mapping $I_0(\mathbf{x})$ to $I_1(\mathbf{x})$ that acts in the following (nonlinear) fashion:

$$I_1(\mathbf{x}) = I_0(\mathbf{x} + T(\mathbf{x})). \tag{1.2}$$

Instead of relying on the tangent space, that accounts only for infinitesimal transformations, nonlinear transport operators allow a greater deal of motion on the manifold and are not limited by linearity assumptions. A key factor distinguishing the linear and nonlinear approaches is the intrinsic feature of transport operators, i.e., transport operators are defined without a specific embedding of the IAM, while previous approaches to IAMs were extrinsic and rely on embeddings. Moreover, we may also use transport operators to study the structure of the IAM via the effects of the parameters that generated the IAM, apart from its apparent geometric properties. Finally, in case the IAM comes with additional

algebraic structure, for instance if the IAM was generated by affine motions or more generally a Lie group, appropriate transport operators have analytic expressions in terms of the generators of the Lie group and the associated Lie algebra via matrix exponentials and various methods have been proposed to estimate the model parameters [6, 13, 19, 27].

As an example, consider an IAM generated by affine transformations so that the parameter space can be identified with the group $\mathbb{R}^2 \rtimes GL_2(\mathbb{R})$. The corresponding transport operator takes the form

$$I_1(\mathbf{x}) = I_0(A\mathbf{x} + b) \tag{1.3}$$

where the model parameters $A \in GL_2(\mathbb{R}), b \in \mathbb{R}^2$ are specific to the IAM and reflect the manifold geometry.

1.4 Optical Flow

As shown in [21], *optical flow* can be viewed as a powerful transport operator on an IAM. Optical flow [4, 10, 24] is a computational method used in estimating the apparent motion of pixels between successive images. Given two images I_0 and I_1, the optical flow between them is defined to be the tuple $(\mathbf{v}_x, \mathbf{v}_y)$ such that

$$I_1(x, y) = I_0(x + \mathbf{v}_x(x, y), y + \mathbf{v}_y(x, y)). \tag{1.4}$$

A common method of computing the pair $(\mathbf{v}_x, \mathbf{v}_y)$ involves solving the partial differential equation obtained by linearizing the above equation as

$$I_1(x, y) = I_0(x, y) + \nabla_x I_0 \mathbf{v}_x(x, y) + \nabla_y I_0 \mathbf{v}_y(x, y) \tag{1.5}$$

where $\nabla_x I_0, \nabla_y I_0$ are the image gradients [4, 10, 24]. In the context of IAMs, optical flow is best viewed as a *smooth operator* that transforms one image into another. Specifically, the collection of *all* optical flow operators at a point on an IAM is empirically known to be a manifold of the same dimension as the IAM [21] and comes with a metric that reflects the parameter changes between images. Moreover, this new operator manifold (called an optical flow manifold or OFM) can be used to obtain a canonical atlas for the IAM. To see the efficacy of optical flow as a transport operator, consider the case of image interpolation again, where now optical flow is used as the transport operator (see Fig. 1.3). Here, the path generated on the IAM via optical flow operators is a better representative of a path on the IAM, i.e., the intermediate points lie on the IAM. Moreover, if the IAM is generated via Lie group actions, then this path coincides with the geodesic path.

1.5 Our Contributions

The main aim of this thesis is to develop the mathematical framework to analyze *transport operators* on IAMs, with optical flow being the candidate transport operator. Our main contribution is the development of analytic tools for an a priori data-driven application. We develop tools for IAMs that mirror the differential geometric tools applied in statistical

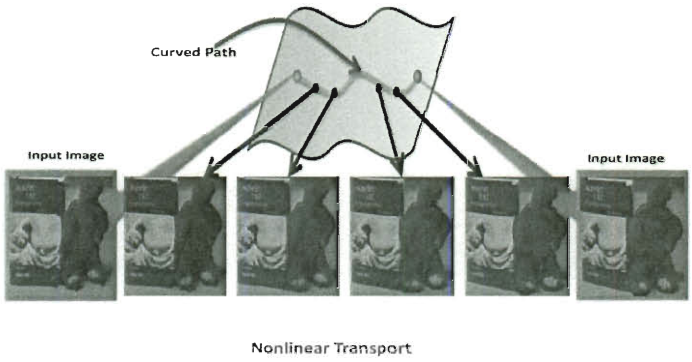

Figure 1.3: Optical flow based transport on IAMs. This nonlinear transport on the IAM provides a more accurate path between the two input images. Moreover, if the IAM is generated via Lie group actions, then the path generated coincides with the geodesic path.

shape theory [12, 15, 22, 23, 26, 28, 31] etc.

We describe the notion of optical flow manifolds (OFMs) as being "non-linear tangent spaces" consisting of transport operators at each point on the manifold. We are guided by the empirical results of [21] that indicate that the OFMs are well-behaved and in particular, are smooth manifolds of the same dimension as the IAM. Moreover, each OFM has a natural metric which is locally isometric to the corresponding parameter values. Using this as our starting point, we consider the induced metric on the IAM which we dub the *flow metric* and show that the flow metric between two points of the IAM is a measure of the distance between the corresponding *parameter values*, thereby introducing a new, more sensible metric for IAMs. The development of the flow metric on the IAM then allows us to consider the application of parameter estimation on the IAM, and we show how the OFM framework includes previous algebraic methods.

Using the flow metric, we characterize the effect of transport operators on the IAM and

in turn develop analytic notions such as optical curvature, optical flow fields and parallel transport. We analyze in detail the case of optical flow fields defined along a fixed curve. In particular, we define a unique function associated to each such flow field, which we dub the *motion function*, using which we can define the notion of *parallel* flow fields. We answer the natural question of how one can optimally approximate a non-parallel field by a parallel field, and thereby induce uniform motion along the curve. We also construct a monoid structure on the set of all flow fields along the curve, and under certain curvature conditions on the curve, the space of parallel optical flow fields is a submonoid that also comes with a convenient multi-scale structure.

The remainder of the thesis is organized as follows. In chapter 2, we introduce optical flow manifolds (OFMs) and using a fixed metric on the OFMs, we study the induced flow metric on the corresponding IAM. Using the flow metric, we develop geometric tools such as optical radius, curvature etc. on the IAM in chapter 3 and highlight the application of these ideas to parameter estimation. We also develop error bounds on approximating non-parallel flow fields by parallel flow fields and illustrate the idea with the example of video resampling. In chapter 4 we develop the multiscale structure of parallel flow fields. We conclude in chapter 5 with a brief discussion.

Chapter 2

Optical Flow Manifolds

In this section, we define the notion of optical flow manifolds (OFMs) corresponding to an IAM $\mathcal{M}$. We show that OFMs are smooth manifolds consisting of optical flow transport operators defined at each point of the correspond IAM and hence can be viewed as "nonlinear tangent spaces" [21]. First, we review the basic facts regarding IAMs and the imaging process.

2.1 IAMs and the Imaging Process

The generation of an IAM $\mathcal{M}$ from the parameter space Θ is a two step process: first the parameter space acts on a three dimensional object or scene and the corresponding object/scene is imaged. Mathematically, we represent this as an imaging map $i : \Theta \to \mathcal{M}$ that takes the parameter $\theta \in \Theta$ to the corresponding two dimensional image $i(\theta)$ (see [14] for a detailed discussion on image formation). The imaging map i controls the geometry of the IAM: A bijective i implies all the structure in the parameter space is transferred to the IAM. A non-bijective i implies that the object has symmetries and these symmetries are reflected in the structure of the IAM.

As motivation for future developments, we now consider the case of of Θ having the structure of a Lie group (i.e., Θ is itself a smooth manifold with the algebraic structure of a group). For instance, parameter spaces such as translations, rotations, homographies etc. fall into this category. The corresponding IAM M can then be thought of as a space obtained from Θ as follows. Considering a fixed object $\mathcal{O}$, we see that Θ acts on the object $\{\mathcal{O}\}$ to generate the orbit of all possible object orientations denoted by $\mathcal{S}_{\mathcal{O}}$.

$$\mathcal{S}_{\mathcal{O}} = \{\theta \bullet \mathcal{O} : \theta \in \Theta\}, \tag{2.1}$$

where $\theta \bullet \mathcal{O}$ indicates the action of θ on $\mathcal{O}$. Moreover, the object at any orientation can be obtained from $\mathcal{O}$ by the action of an appropriate $\theta \in \Theta$. This action can be used via the imaging map i to define a transitive action $\tilde{f}$ of Θ on the corresponding IAM

$$\tilde{f} : \Theta \times M \to M. \tag{2.2}$$

Therefore the entire IAM can be realized as $M = \Theta/\Lambda$ with Λ being the isotropy subgroup in Θ consisting of all $\theta \in \Theta$ fixing the image $I_{\mathcal{O}}$ corresponding to object $\mathcal{O}$.

As an example, consider a uniformly colored 3D sphere $\mathcal{O}$ undergoing rotation about a fixed axis (see Fig. 2.1). Here, the parameter space Θ is the unit circle, S^1 which has the structure of a Lie group. Being uniformly colored, the sphere does not change appearance under rotation, and we see that the isotropy subgroup $\Lambda = S^1$ as the action is trivial, and hence, the IAM degenerates to a single point $\{I_{\mathcal{O}}\}$. Had the sphere been textured, we obtain

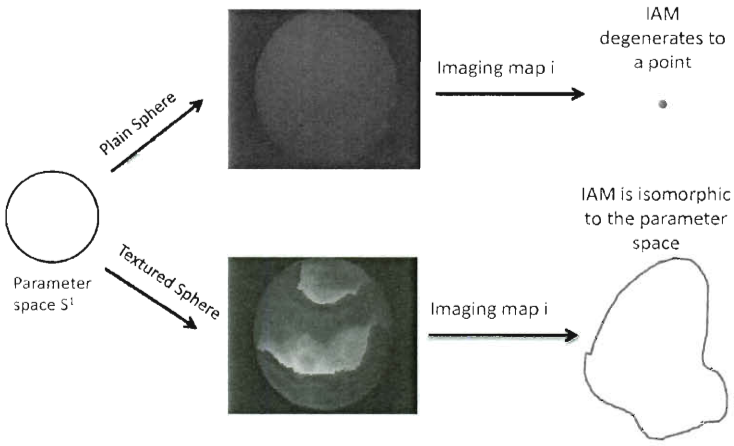

Figure 2.1: The IAM of a plain sphere upon one dimensional rotation degenerates into a point as the sphere provides no additional information while rotating. A textured sphere provides new views upon rotation and hence its IAM is isomorphic to the circle S^1.

new views of the sphere for each rotation and hence see that Λ is the trivial subgroup so that the IAM is isomorphic to S^1. The degeneracy of the plain sphere is due to the non-injectivity of the imaging map i while the textured sphere has an injective imaging map. For the remainder of the thesis, we will consider IAMs without degeneracies by assuming that the imaging map i is injective.

We thus see how the dimensionality and structure of the IAM is dependent on the parameter space and imaging map. Therefore, any reasonable tool for analyzing IAMs *must* take the parameter space into account. As we have seen, optical flow does precisely that, i.e., the optical flow between two images on an IAM measures the apparent motion between the two images and is thus provides direct access to the corresponding parameter change between the two images.

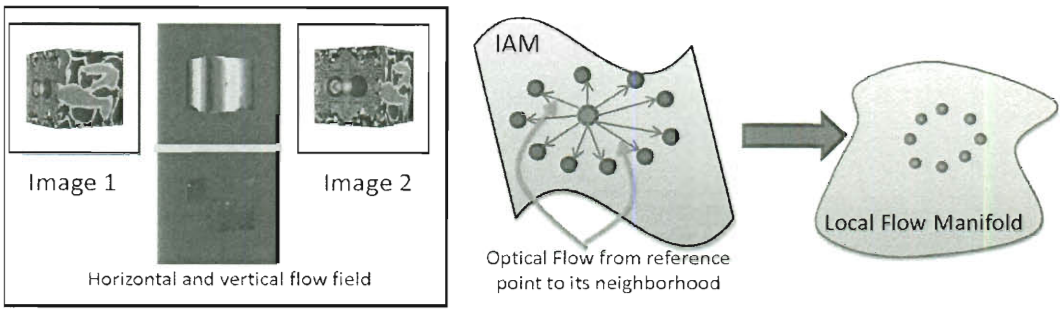

Figure 2.2: A pictorial representation of OFMs. We compute the optical flow between a base image and its neighbors. The space of such flow operators is the OFM at the base image, or the local flow manifold.

2.2 Optical Flow Manifolds

For a fixed base image $m \in M$, consider a neighborhood $N(m)$ of m. If for $m' \in N(m)$, there are flow vectors $(\mathbf{v}_x, \mathbf{v}_y)$ such that m' can be obtained from m using the flow vector, i.e., $m'(x, y) = m(x + \mathbf{v}_x(x, y), y + \mathbf{v}_y(x, y))$, we say that optical flow exists from m to m'. We denote this as $\phi_{\mathbf{v}_x, \mathbf{v}_y}(m) = m'$ or simply $\varphi(m) = m'$. In practice, occlusion or boundary effects may lead to undefined estimates for the flow vectors. However, as described in [21], one can mitigate these issues by incorporating additional consistency tests to ensure that only the meaningful flow vectors are retained.

This is illustrated in Fig. 2.2. Here, the IAM is two dimensional and is generated by rotating a textured cube in two dimensions. Image 1 is the base image and Image 2 is a neighbor. We compute the horizontal and vertical flow vectors between Image 1 to Image 2 and this pair of flows is a *point* on the OFM at Image 1.

The set of all points $m' \in M$ for which optical flow from $m \in M$ to m' exists is a neighborhood of m, which we denote by B_m, i.e.,

$$B_m = \{m' \in M : m'(x, y) = m(x + \mathbf{v}_x(x, y), y + \mathbf{v}_y(x, y))\}.$$

Using this neighborhood, we define the optical flow manifold O_m at m to be the corresponding set of optical flows ϕ between m and points in B_m, i.e.,

$$O_m = \{\phi = (\mathbf{v}_x, \mathbf{v}_y) : \phi(m) \in B_m\}.$$

Note that we have always the trivial flow ϕ_0 such that $\phi_0(m) = m$. Moreover, O_m is nonlinear, i.e., the algebraic sum of two flows is not a meaningful flow. It is clear that the collection of neighborhoods $\{B_m : m \in M\}$ forms a base for the manifold structure of M.

Proposition 1. *Let M be a K dimensional IAM. Then O_m has the structure of a manifold homeomorphic to B_m.*

Proof. We first show that O_m is homeomorphic to B_m and pullback the smooth structure of B_m to induce a smooth structure on O_m. Consider the map $g : B_m \to O_m$ that sends a point $m' \in B_m$ to $\phi \in O_m$ such that $\phi(m') = m$. g is clearly bijective and hence, we use g to endow O_m with the quotient topology. Moreover, as g is injective, g is a homeomorphism as g is an open map: given an open set $U \subset B_m$ we have $U = g^{-1}(g(U))$ and by the quotient topology on O_m, we have that $V = g(U)$ is open in O_m as $g^{-1}(V) = U$ is open in B_m. As $\{B_m : m \in M\}$ is a base for the manifold structure of M, there exists continuous maps $\{\Phi_m : m \in M\}$ so that $\{(B_m, \Phi_m) : m \in M\}$ is an atlas for M. Therefore, the composition $\Phi_m \circ g^{-1}$ is a homeomorphism from O_m to an open set W in $\mathbb{R}^K$. As O_m is now covered by the single chart $\{O_m, \Phi_m \circ g^{-1}\}$, we can pullback this smooth to O_m via $\Phi_m \circ g^{-1}$ and endow O_m with a smooth structure. Moreover, B_m is homeomorphic to O_m by construction. □

Definition 2. *Let M be a K dimensional IAM. The manifold O_m is called the* Optical Flow Manifold *(OFM) at $m \in M$. The neighborhood B_m is called the* optical neighborhood *around m.*

We make a few preliminary observations. First, by the homeomorphic relationship between O_m and B_m, we conclude that O_m is also a K dimensional manifold. Also, O_{m_1} is homeomorphic to O_{m_2} for any $m_1, m_2 \in M$. Moreover, the distinguished element $o_0 \in O_m$ for each $m \in M$ that maps m to itself in B_m acts a natural "origin" in O_m.

Next, we observe, again from the homeomorphic relationship between B_m and O_m, that given any point $m_1 \in B_m$ there is a unique operator o_1 such that $o_1(m) = m_1$. A question to ask is whether there is any relationship between O_m and the tangent space T_m at m. Indeed, for a smooth IAM, one can define tangent spaces T_m at $m \in M$ and the OFM O_m at m is diffeomorphic to a neighborhood of $0 \in T_m$. To see this fact, recall that the *exponential map* defined on T_m is a diffeomorphism between a neighborhood U_0 of $0 \in T_m$ and a neighborhood of V_m of m. We also have a diffeomorphism Φ from O_m to B_m by definition. Now, B_m is open and there is an open ball $B_0 \subseteq U_0$ on which $\Phi^{-1} \circ exp$ is a diffeomorphism, being a composition of two diffeomorphisms.

As a concrete example, consider again the case of the IAM generated by imaging a translating black disk on an infinite white background. We will denote this IAM by M_T. Note that the parameter space in this case is $\Theta = \mathbb{R}^2$. Also, as there is no occlusion between any two images on M_T, it follows that given any $m, m' \in M_T$, there exists a $o \in O_m$ such that $o(m) = m'$. As this is true for any pair of images in M_T, we conclude that $O_m = \mathbb{R}^2$

$\forall m \in M_T$ and hence, $B_m = M_T \; \forall m \in M_T$. More generally, we note that for an IAM M generated by Lie group actions without occlusion between images, the OFM O_m at any point $m \in M$ can be identified with the parameter space Θ and neighborhood B_m at each point is the entire manifold M. As a corollary, one can recover the geodesic path between two any two points $m, m' \in M$ by using appropriate flow operators in O_m to generate the geodesic path from m to m'. We will return to these examples in future sections and show how our more general formulation contains the algebraic methods such as [6, 13, 19, 27] as special cases.

The smoothness of each OFM indicates that OFMs are better objects to work with rather than the original IAM. For instance, common dimensionality reduction methods such as [2, 20, 25] etc. assume that the manifold is smooth, and hence, are tools that can be profitably applied to OFMs. This is indicated in Fig. 2.3. Here, we see that the pairwise distance between points on a given OFM varies very smoothly, as opposed to the IAM, where due to sharp edges, the matrix of pairwise distance has large off-diagonal entries. Moreover, the residual error of embedding the OFM into Euclidean space decays very rapidly, while embedding the IAM into Euclidean is suffers from errors. As a result, we see that it is easier to analyze the collection of OFMs at different points on the IAM as opposed to the IAM itself.

As in the case of the tangent bundle, we can construct an analogous bundle with the collection of O_m as m varies through M:

Definition 3. *Let M be an IAM and O_m the OFM at $m \in M$. We define the* flow bundle

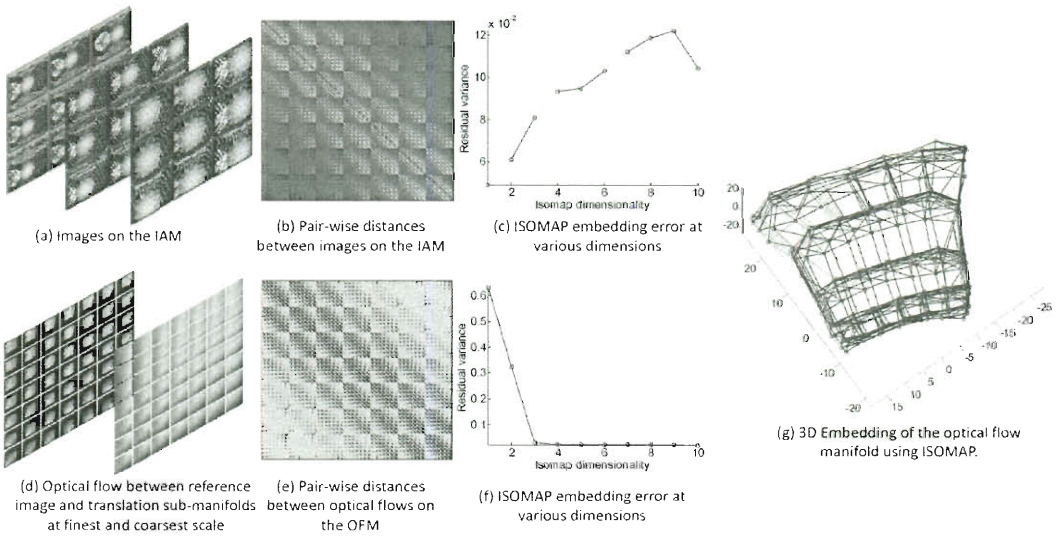

Figure 2.3: Comparison of manifold processing on a 3D IAM generated by translating and scaling a reference image (top) and a fixed OFM (bottom).(a) Sample points on the IAM. (b) Pairwise distances on the IAM. The relatively large off-diagonal entries corresponding to the IAM indicated the lack of local isometry to Euclidean space and non-differentiability of the IAM (here, red values indicate large entries and blue values indicate small entries). As a consequence, dimensionality reduction methods such ISOMAP in this case work badly on the IAM as shown in (c). (d) Points on a fixed OFM. (e) The pairwise distance matrix corresponding to the OFM indicates that the OFM is close to being locally isometric to Euclidean space, yielding perfect embedding as shown in (f) and (g).

OM on M to be the disjoint union of the O_m as m varies over M, i.e.,

$$OM = \coprod_{m \in M} O_m.$$

Thus, an element of OM is a pair (m, ϕ) with $\phi \in O_m$. Using this fact, we can induce a topology on the flow bundle.

Proposition 4. *Given a K-dimensional IAM M, the flow bundle OM is a $2K$-dimensional manifold.*

Proof. We first note that if $(m, \phi) \in OM$ then $\{m, \phi(m)\} \in \{m\} \times B_m$. Thus, given an atlas $\{(U_\lambda, \psi_\lambda)\}_{\lambda \in \Lambda}$ of M, we have that

$$\psi^{\star}_{\alpha,\beta}((m,\phi)) = (\psi_\alpha(m), \psi_\beta(\phi(m)))$$

maps (m,ϕ) into $\psi_\alpha(U_\alpha) \times \psi_\beta(U_\beta \bigcap B_m)$ where U_α and U_β are charts around m and $\phi(m)$ respectively. The (continuous) inverse of $\{x_1,...,x_k,y_1,...,y_k\} \in \psi_\alpha(U_\alpha) \times \psi_\beta(U_\beta \bigcap B_m)$ is given by (m,ϕ) where $\psi_\alpha(m) = \{x_1,...,x_k\}$ and ϕ is the unique operator in O_m such that $\psi_\beta(\phi(m)) = \{y_1,...,y_k\}$ so that OM is locally Euclidean. □

Thus, we see that OFMs are manifolds consisting of flow operators that are defined pointwise on the corresponding IAM. The action of flow operators at a base point on the IAM results in motion *along* the IAM, as opposed to linear transport that results in motion *off* the manifold. Our next objective will be to use define appropriate distances on the IAM via certain natural metrics on the collection of OFMs.

2.3 Metric Structure on the IAM via the Metric on the OFMs

Consider again the translational manifold M_T, where the OFM O_m at each point $m \in M_T$ can be identified with $\mathbb{R}^2$. Being isometric with $\mathbb{R}^2$, we can endow each O_m with the Euclidean metric which we denote as $d_O(\cdot,\cdot)$. Let $\theta_1, \theta_2 \in \mathbb{R}^2$ be a pair of parameters such that $m_1 = i(\theta_1), m_2 = i(\theta_2)$; note that there exists a $\phi \in O_{m_1}$ such that $\phi(m_1) = m_2$. It then follows that $d_O(\phi_0,\phi) = C'\|\theta_1 - \theta_2\|$ for some $C' > 0$. In particular, $d_O(\cdot,\cdot)$ is locally isometric to the corresponding parameter values. This is illustrated in Fig. 2.4. As the empirical results of [21] indicate, the above discussion holds analogously for generic OFMs, i.e., each O_m has an associated metric $d_O(\cdot,\cdot)$ and this metric is locally isometric to the corresponding metric on the parameter space Θ. We indicate this as

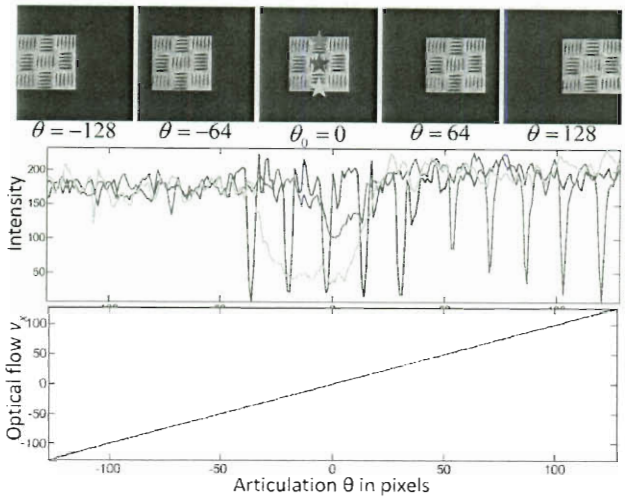

Figure 2.4: A comparison of pixel intensity variations and optical flow variations at three landmark pixels (in stars) as a function of the parameter values for the translational manifold. We see that the intensity of pixels across different parameter values changes rapidly, and hence, computing the distance between images using intensity differences is a not a good metric for measuring parameter changes. On the other hand, the optical flow between two images is a linear function of the parameter values, and hence is an excellent metric to measure parameter changes.

$$d_O(\phi_0, \phi) \propto d_\Theta(\theta_1, \theta_2).$$

Our main focus in the remainder of this section is to define a corresponding metric on an arbitrary IAM M obtained from the metric $d_O(\cdot, \cdot)$ on O_m such that the resulting metric on M also has the property of being locally isometric to the changes in parameters. As a first step, we locally "push forward" the metric on O_m onto B_m as follows. For points $m_1, m_2 \in M$ with $m_2 \in B_{m_1}$, we have a unique operator ϕ_1 such that $m_2 = \phi_1(m_1)$ so that we can define the distance $d_M(m_1, m_2)$ as the corresponding distance between ϕ_0 and ϕ_1, i.e.,

$$d_M(m_1, m_2) := d_O(\phi_0, \phi_1). \tag{2.3}$$

Moreover, if $m_1 = f(\theta_1)$ and $m_2 = f(\theta_2)$, for parameters $\theta_1, \theta_2 \in \Theta$ we have

$$d_M(m_1, m_2) \propto d_\Theta(\theta_1, \theta_2). \tag{2.4}$$

However, this definition does not readily extend to the case where m_1 and m_2 are not "optically related", i.e., $m_2 \notin B_{m_1}$. In this case, we first connect m_1 and m_2 by a path c such that $c(0) = m_1, c(1) = m_2$. We then partition the domain of c by a partition $P = \{0 = t_0 < t_1 < \cdots < t_n = 1\}$ such that the intermediate points along the path are optically related i.e. $c(t_i) \in B_{c(t_{i-1})}$, where we assume for a fine enough partition, we can obtain such a nesting. We then define the distance along c to be

$$d(c, m_1, m_2) = \sup_P \sum_{i=0}^{n-1} d_M(c(t_i), c(t_{i+1})), \tag{2.5}$$

where the supremum is over all partitions of the path and distance $d_M(\cdot, \cdot)$ is as mentioned in equation 2.3. By taking the infimum over all possible paths, we obtain a metric on M, i.e.,

$$d_M(m_1, m_2) = \inf_c \sum_{i=0}^{n-1} d_M(c(t_i), c(t_{i+1})). \tag{2.6}$$

In essence, the metric $d_M(\cdot, \cdot)$ is similar to the Riemannian distance: first we define distance over a fixed curve, and then take the infimum over all possible paths.

Proposition 5. *For an IAM M, the distance $d_M(\cdot, \cdot)$ 2.3 is a metric on M.*

Proof. Positivity of $d_M(\cdot, \cdot)$ is clear, moreover, $d_M(m, m) = 0$. If $m_1 \neq m_2$, then for

every path c between m_1 and m_2, we have that $\sum_{i=0}^{n-1} d_M(c(t_i), c(t_{i+1})) \neq 0$ and hence, $d_M(m_1, m_2) \neq 0$. Symmetry follows from the fact that along c, $c(t_i) \in B_{c(t_{i-1})}$ and hence, $d_M(c(t_i), c(t_{i+1})) = d_M(c(t_{i+1}), c(t_i))$. For the triangle inequality, we note that given paths c_1 and c_2 from m_1 to m_2 and m_2 to m_3 respectively, the path $c_1 * c_2$ obtained by traversing c_1 and c_2 in succession at twice the rate (i.e. $c_1 * c_2(t) = c_1(2t)$ for $0 \leqq t \leqq \frac{1}{2}$ and $c_1 * c_2(t) = c_2(2t-1)$ for $\frac{1}{2} \leqq t \leqq 1$) is a path from m_1 to m_3 and $\sum_{i=0}^{n-1} d_M(c_1(t_i), c_1(t_{i+1})) + \sum_{i=0}^{n-1} d_M(c_2(t_i), c_2(t_{i+1})) \geqq \sum_{i=0}^{n-1} d_M(c_1 * c_2(t_i), c_1 * c_2(t_{i+1}))$. By taking the infimum over all such paths, we verify the triangle inequality. □

Recall that the metric on O_m satisfies $d_O(\phi_0, \phi) \propto d_\Theta(\theta_1, \theta_2)$ with $o \in O_m$ and θ_1, θ_2 being the parameters corresponding to m and $o(m)$ respectively. From the above result, we see that with the metric $d_M(\cdot, \cdot)$ on M, we have

$$d_M(m_1, m_2) \propto d_\Theta(\theta_1, \theta_2) \tag{2.7}$$

where m_1 and m_2 are points on M corresponding to the parameter values θ_1 and θ_2 respectively under the assumption that the monotonicity of $d_O(\cdot, \cdot)$ over different O_m is universal, i.e., it does not change between different optical neighborhoods. We refer to this metric on M as the *flow metric*. We can now state the main result of this section that follows from the above discussion.

Theorem 6. *Let M be an IAM and let $d_M(\cdot, \cdot)$ be the associated flow metric. Then, $d_M(m_1, m_2) \propto d_\Theta(\theta_1, \theta_2)$ with m_1 and m_2 being points on M corresponding to the pa-*

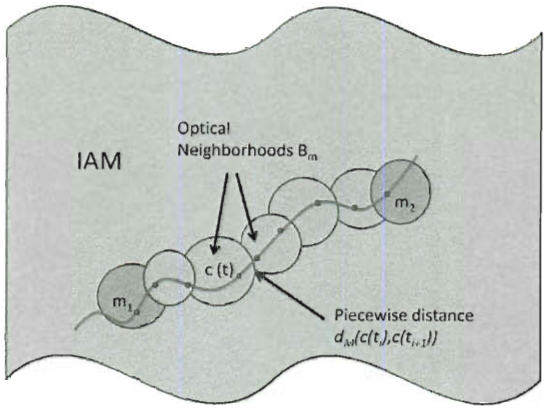

Figure 2.5: A pictorial representation of OFMs and the flow metric. Each OFM is mapped homeomorphically onto the optical neighborhood B_m of the corresponding base point. The optical flow distance between two points is computed by considering the infimum over all possible curves of the piecewise flow distance $d_M(c(t_i), c(t_{i+1}))$.

rameter values θ_1 and θ_2 respectively.

2.3.1 Application: Parameter Estimation:

Let $m \in M$. We consider the problem of estimating $\theta \in \Theta$ such that $i(\theta) = m$ given a finite number of template points $m_1, \cdots, m_n \in M$ with neighborhoods $B_{m_1}, \cdots B_{m_n}$ that cover M. As a motivating special case, consider first the situation when $M = M_T$, the translational manifold with $\Theta = \mathbb{R}^2$ and a single template point m'. A similar problem has been dealt with in [6, 19] where the authors estimate the Lie group generators corresponding to the IAM. Given the parameter value $\theta' = (c'_1, c'_2)$ of the base image m', we can compute the the parameter θ corresponding to m as follows. First, we find the unique flow operator $\phi = (\phi_1, \phi_2) \in \mathbb{R}^2$ such that $\phi(m') = m$. The parameter value θ corresponding to m is then obtained as $\theta = (c'_1 + \phi_1, c'_2 + \phi_2)$. An entirely similar result hold for generic IAMs generated by Lie group actions. From this simple example, we see that finding the

optimal θ is equivalent to finding the optimal flow operator ϕ that minimizes $d_M(\phi(m'), m)$ with $\phi \in O_{m'}$. We return to the general case with n template images and seek the optimal flow operator $\phi \in O_{m_i}$ that minimizes $d_M(\phi(m_i), m)$, $i = 1, \cdots, n$. Here, a single neighborhood does not cover the entire IAM and hence, to estimate ϕ, we first find the neighborhood $B_{\tilde{m}} \in \{B_{m_1}, \cdots B_{m_n}\}$ such that $\tilde{m} = \arg\min_{m' \in \{m_1, \cdots, m_n\}} d_M(m, m')$. Our search is then restricted to the neighborhood $B_{\tilde{m}}$. Within this neighborhood, we find the optimal $\phi \in O_{\tilde{m}}$ as before, i.e., $\hat{\phi} = \arg\min_{\tilde{\phi} \in O_{\tilde{m}}} d_M(\tilde{\phi}(\tilde{m}), m)$. In essence, we first find the optimal template point and then search within the corresponding OFM for the optimal flow operator. If a single template point generates the entire IAM, this general procedure clearly reduces to the Lie group case discussed earlier. We thus see that the generic OFM formulation includes the algebraic methods of [19, 27] as a special case.

The remainder of the thesis is devoted to developing geometric tools for IAMs leveraging the flow metric. Note that, unlike the tangent space, the OFM has no linear structure and hence, we do not have at our disposal tools such as parallel translation, covariant derivatives etc. We will construct analogous tools for our purposes via the flow metric and hence open up a new view of IAM analysis via using the flow metric.

Chapter 3

Geometric Tools for IAMs via the Flow Metric

In this section, we develop basic tools to analyze the structure of IAMs using the flow metric. We will pay special attention to flow operators defined along curves on the corresponding IAMs. Keeping computations in mind, these tools will open the door to a variety of applications as mentioned in the introduction and beyond.

3.1 Local Properties: Flow Radius

We first seek an appropriate measure of the size of an OFM and the corresponding optical neighborhood.

Definition 7. *Given an IAM M and $m \in M$ we define the* flow radius *or simply the* radius *r_m at m as*

$$r_m = \sup_{n \in B_m} d_M(m, n).$$

Note that we may regard r_m as a function from M to $\mathbb{R}^+$ i.e. $r(m) = r_m$ is a map from M into the non-negative reals. Moreover, it is continuous as a function of m. Consider the variations of r_m as m varies. If r_m is large, then one can find a suitable operator $o \in O_m$ that transports m to a far away point, with distance measured using the flow

metric. Conversely, a small r_m indicates that m can only be transported within a small region, or said differently, m obstructs transport on the IAM. Moreover, rapid changes in the magnitude of r_m within a small neighborhood indicate that the manifold is not well-behaved near m: there are several points close to m that obstruct transport while there are also several points that allow flow over large distances on the IAM.

3.2 Flow radius and Lie groups

A class of IAMs for which r_m is very well behaved, indeed for which r_m is a constant, are those generated by a Lie group action. As a motivating example, consider again the translational manifold M_T. We note that as $O_m = \mathbb{R}^2$ for each $m \in M_T$, it follows that $r_m = \infty$. If the parameter space Θ is compact, for instance, if $\Theta = S^1$ and we consider affine rotations of a base image m generating the IAM M, then we again have that $B_m = M$ and r_m is a constant $0 < c < \infty$. For a generic IAM M generated by Lie group actions with $B_m = M$, it follows that the flow radius is a constant whose exact value depends both on the object being imaged as well as the nature of the imaging parameter.

3.3 Optical Curvature

The above discussion indicates that the ratio $\frac{1}{r_m}$ is a measure of "optical curvature". If r_m is large (or infinite), then the IAM is can be thought as being "optically flat" at m in the sense that there is no obstruction to transport on the manifold at m. In the other limiting case, i.e., if r_m approaches zero, the only operator in O_m is the trivial operator o_0

and hence, M is has high "optical curvature" at m. We thus have the following definition:

Definition 8. *Given an IAM M and $m \in M$ we define the* optical curvature *or simply the* curvature *at m as $K_m = \frac{1}{r_m}$.*

While the traditional notion of curvature is a point property, the optical curvature we have defined depends on both the base point as well as the neighborhood properties. In terms of optical curvature, we can now state that if M is generated by a Lie group Θ then, M has constant optical curvature. The class of IAMs with constant optical curvature will play a prominent role in our later analysis.

3.4 Optical Flow Fields

In this section, we will focus on a construct motivated by differential geometry, namely the idea of a vector field on a manifold. Recall that a vector field is a *section* of the the tangent bundle, i.e., a vector field is a map $\sigma : M \to TM$ such that $\pi \circ \sigma = id_M$ where π is the natural projection from the tangent bundle and id_M is the identity map on M. In an analogous fashion, an *optical flow field*, or simply an *optical field*, is defined as a section of the *optical flow bundle* of M.

While vectors fields are defined generically on manifolds, the special class of vector fields along curves is especially important in differential geometry. Vector fields along curves give rise to tools such as parallel translation, Jacobi fields, etc. [8]. In the case of IAMs, which lack analytic structure in general, we will define optical fields along curves on an IAM and recover similar geometric tools using the flow metric. As we assign operators

to points on the curve, we intuitively would like the transport induced by the operator to remain along the curve so that the collection of flow operators induces *motion* along the curve. This special class of optical fields will be our main object of study for the rest of the thesis.

Definition 9. *Let M be an IAM and c be a smooth curve passing through $m_1, m_2 \in M$.Define $B_{c(t)} \bigcap c = \{c(t') \in O_{c(t)} : t' \geq t\}$. An* optical field from m_1 to m_2 along c *with $m_1, m_2 \notin \partial c$ is a map $V : t \mapsto OM$ such that $V(t) := V_t \in O_{c(t)}$ and $V_t(c(t)) \in \overline{B_{c(t)} \bigcap c}$ where by $V_t(c(t))$ we mean the point on the curve obtained by the action of V_t on $c(t)$.*

In other words, an optical field along c is an assignment of a flow operator V_t with V_t an element of the OFM at $c(t)$ such that such that the action V_t on $c(t)$ remains on the curve. Thus, the action of V_t on the base point $c(t)$ at time t induces motion along the curve. When m_1 and m_2 are clear from the context, we simply refer to V_t as a optical field along c.

In essence, the curve V_t traces a curve in OM as t varies with a consistent action on $c(t)$. Note that by $B_{c(t)} \bigcap c$ we mean the intersection of the K dimensional optical neighborhood $B_{c(t)}$ with the one dimensional curve c starting at $c(t)$ and hence, $B_{c(t)} \bigcap c$ is a one dimensional embedded curve in $B_{c(t)}$ i.e., $B_{c(t)} \bigcap c$ is a one dimensional "slice" of $B_{c(t)}$.

To measure the distance traveled by the action of V_t on $c(t)$, we define a radius r_t restricted along the curve that measures distance along c as opposed to the complete flow radius $r_{c(t)}$ at $c(t)$.

$$r_t = \sup_{n \in B_{c(t)} \bigcap c} d_c(c(t), n),$$

where $d_c(\cdot,\cdot)$ is the flow metric restricted to the curve c. Likewise, the curvature K_t along c is the ratio

$$K_t = \frac{1}{r_t}.$$

As $B_{c(t)} \bigcap c$ is one dimensional, the distance $d_c(c(t), m)$ between $c(t)$ and $m \in B_{c(t)} \bigcap c$ characterizes m in the following sense. Given any positive constant $0 \leq \eta \leq r_t$ there is a unique $m \in B_{c(t)} \bigcap c$ with $d_c(c(t), m) = \eta$. Thus, by specifying the distance along the curve c, we effectively characterize the curve. Lifting this observation into $O_{c(t)}$, we have the following result.

Theorem 10. *Let M be an IAM, c be a curve passing through $m_1, m_2 \in M$, and V_t be an optical field from m_1 to m_2 along c. Then, V_t is completely characterized by the function $h_V(t) = d_c(V_t(c(t)), c(t))$ in the sense that for any non-negative function $h(t)$ bounded pointwise by r_t, there exists a unique optical optical field V_t such that $h_V(t) = h(t)$.*

Proof. That $0 \leq h_V(t) \leq r_t$ is clear from the definitions above. Let $h(t)$ be any non-negative function bounded by r_t. Then, for fixed $t = t_0$ we have that $0 \leq h(t_0) < r_{t_0}$. By the remark made previously, we have a unique $m_{t_0} \in B_{c(t_0)} \bigcap c$ with $d_c(c(t_0), m_{t_0}) = h(t_0)$. Now, as $m_{t_0} \in B_{c(t_0)} \bigcap c$, in particular, $m_{t_0} \in B_{c(t_0)}$ and hence there exists a unique $o_{t_0} \in O_{c(t_0)}$ such that

$$o_{t_0}(c(t_0)) = m_{t_0}.$$

As t_0 was arbitrary, as t varies, we can define $V_t = o_t$. Moreover,

$$h_V(t) = d_c(V_t(c(t)), c(t)) = d_c(o_t(c(t)), c(t)) = d_c(m_t, c(t)) = h(t)$$

so that $h(t)$ characterizes V_t. □

Recall that we view an optical flow field V_t along c as a curve in OM. Theorem 10 states that this curve is characterized by the function $h_{V^c}(t)$ in the sense that for a given V_t along the (fixed) curve c, the function $h_{V^c}(t)$ contains all the information about the motion induced by V_t on the curve i.e. $h_{V^c}(t)$ measures the distance to which V_t transports $c(t)$ in $B_{c(t)} \bigcap c$. As this function is of prime importance, we make the following definition:

Definition 11. *Given an optical field V_t along a curve c, we define its* motion function *to be*

$$h_{V^c}(t) = d_c(V_t(c(t)), c(t)).$$

Note that by continuity of the metric $d_c(\cdot, \cdot)$ and $c(t)$, the function $h_{V^c}(t)$ is also continuous.

3.5 Parallel Optical Fields

We have a very natural geometric interpretation of the motion function h_{V^c} of an optical flow field V_t along a curve c. Namely, it is a measure of the distance traveled along the curve at time t by $c(t)$ when acted upon by V_t. Thus, it is natural to think of instantaneous changes in h_{V^c} in t as a measure of the *velocity* of the motion induced by V_t on $c(t)$. In classical geometry, the class of constant velocity curves is especially important: they correspond to uniform motions. Similarly, we will be interested in the class of constant motion functions h_{V^c}. These correspond to optical fields V_t along c that induce uniform motion along c, where by uniform motion, we mean the distance traveled along c is constant for all time.

Another key link with classical differential geometry is the notion of parallel transport (or parallel translation) of tangent vectors [8]. Parallel transport is a key tool in moving tangent vectors from different tangent spaces while preserving direction/orientation along the curve. Parallel transport utilizes the inherent linear structure of the tangent space to define a linear map between tangent on points along the curve. We aim to enable a similar analytic tool for IAMs. However, an immediate stumbling block is the clear lack of *linear structure* in the OFM. We therefore take a different approach to defining parallel translation in the OFM case using motion functions.

To motivate our definition, we recall that a vector field along a curve c on a manifold is *parallel* if its *covariant derivative* along c vanishes. The covariant derivative is in essence a way of differentiating the vector field along c. The relation between parallel translation and parallel vector fields is that given a tangent vector v in the tangent space of a point $c(t)$ on the curve c, it is possible to extend v along c by parallel translation to yield a parallel vector field along c. In the OFM case, we have the motion function of an optical field along c at our disposal and we use it to characterized parallelism of the field along the curve.

Definition 12. *An optical field V_t along a curve c, is said to be parallel if the derivative of its motion function with respect to t is zero, or equivalently, if the motion function is constant along c, i.e., $h_V(t)$ is a constant.*

In all that follows, we will denote by $\Omega(c, m_1, m_2)$ to be the space of all optical fields through m_1 and m_2 along a curve c passing through $m_1, m_2 \in M$. When m_1, m_2 are understood from context, we simply refer to this space as $\Omega(c)$. The subclass of parallel fields

along c will be denoted by $\omega(c)$. A few facts are immediate from the above definition. First, as $h_{V^c}(t) \leq r_t$ for all t, it is clear that if V_t is to be parallel along c, $h_{V^c}(t)$ is a constant h_{V^c} independent of t and $h_{V^c} \leq \inf_t r_t$. Therefore, in the future, we shall suppress the argument t in the motion function $h_{V^c}(t)$ of a parallel flow field. Second, as V_t is characterized by h_{V^c}, we see that for any constant δ such that $0 \leq \delta < \inf_t r_t$, there is a parallel optical field along $c(t)$ such that $h_{V^c} = \delta$. Such a parallel optical field can be obtained, for example, by choosing for each t a flow operator $\phi_t \in O_{c(t)}$ with $d_c(\phi_t(c(t)), c(t)) = \delta$. The existence of such an optical field ϕ_t is guaranteed by the above theorem. Given $\phi \in O_{c_0}$ we would like to extend ϕ throughout the curve to obtain a flow field V_t such that V_t is parallel along c with $h_{V^c} = d_c(\phi(c_0), (c_0))$. The following result allows for such parallel translation of flow operators along a curve.

Proposition 13. *Let M be an IAM and c be a curve through $m_1, m_2 \in M$. Let $\epsilon = \inf_t r_t$. Then, given any $\phi \in O_{c(t_0)}$ with $\delta = d_c(\phi(c(t_0)), c(t_0)) < \epsilon$ there exists a unique parallel optical field along $c(t)$ with $h_{V^c}(t) = \delta$.*

Proof. As $\delta < \epsilon$, in particular $\delta < r_t$. Thus, invoking the previous theorem for the special case of the constant function $h(t) = \delta$, we have the existence of a unique optical field V_t along $c(t)$ such that $h_{V^c}(t) = \delta$. Moreover, as $h_{V^c}(t)$ is constant, V_t is parallel. □

Note that in contrast with the classical case, parallel transport along a curve is dependent on the nature of the flow operator, i.e., an arbitrary flow operator $\varphi \in O_{c_0}$ cannot be parallel translated along c unless $d_c(\varphi(c_0), c_0) < \inf_t r_t$. This constraint is related to the nature of the curve: parallel transport along a curve that contains points with high optical curvature

K_t is limited to those flow operators that induce smaller motion along the curve. Moreover, the possibility of parallel transport of $\phi \in O_{c(t)}$ has a global dependence, i.e., it depends on the curvature of the entire curve, not only the curvature K_t at the point $c(t)$.

Thus, we are naturally led to study those curves for which parallel translation of an operator ϕ at a single point $c(t_0)$ ensures the possibility of parallel translation of operators at any other point on the curve. Clearly, the necessary condition is the invariance of K_t with t and therefore we are led to consider curves for which the curvature K_t is independent of t, i.e., a constant. This special class of curves has a very rich structure that we explore in the following sections.

3.6 Approximation of Arbitrary Flow Fields by Parallel Flow Fields

In this section, we consider the question of approximating arbitrary $V_t \in \Omega(c)$ by elements in $\omega(c)$. Consider an optical field $V_t \in \Omega(c)$ (not necessarily parallel) along a curve c of constant flow curvature. A natural question to ask is how far away is V_t from being parallel, i.e., we look for a "best" approximation of V_t by a parallel field $W_t \in \omega(c)$ along c. To quantify the error in approximation, we consider the following error:

$$e(t) = d_c(V_t(c(t)), W_t(c(t))). \tag{3.1}$$

In other words, $e(t)$ is a measure of how the action of V_t on $c(t)$ differs from the action of W_t on $c(t)$. Note that $e(t)$ is bounded above by $h_{V^c}(t) + h_{W^c}$ as $e(t) = d_c(V_t(c(t)), W_t(c(t))) \leq d_c(V_t(c(t)), c(t)) + d_c(c(t), W_t(c(t))) = h_{V^c}(t) + h_{W^c}$.

While $e(t)$ is a pointwise error, we need an error that is obtained over the entire curve c. To this end, a natural choice of error metric is:

$$E(V, W) = \int_a^b e(t)dt, \tag{3.2}$$

where the domain of c is the interval (a, b). Thus, our question is to find a parallel optical field $W_t \in \omega(c)$ that minimizes $E(V, W)$, i.e.,

$$W^* = \arg\min_W E(V, W). \tag{3.3}$$

In general, the minimizer may not exist, or may not be unique if one exists. However, the greatest issue is the strong dependence of the error $e(t)$ on the flow metric, that prevents a generic solution to the minimization problem as we cannot infer the convexity of the problem as stated. We can however, obtain a universal lower bound on the error independent of the flow metric as follows:

$$|h_V(t) - h_W| = |d_c(V_t(c(t)), c(t)) - d_c(W(c(t)), c(t))| \leq e(t). \tag{3.4}$$

Therefore, we seek a minimizer of $\int_a^b |h_V(t) - h_W|dt$. Note that as W_t is parallel, h_W is a constant, say $h \geq 0$. Moreover, as c is a path of constant flow curvature, r_t is a constant $r > 0$. As h characterizes W_t, a minimizer h^* yields a lower bound for $E(V, W)$. Our goal then, is to find an optimal constant h^* that minimizes $\widetilde{E(h)} = \int_a^b |h_V(t) - h|dt$. We claim that a solution h^* is a certain "median" of $h_V(t)$. We first define $A_k = \{t \in (a, b) :$

$h_1(t) > k\}$ and $B_k = \{t \in (a,b) : h_1(t) \leq k\}$ for some k. We claim that an optimal constant $\hat{h}$ is such that $\lambda(A_{\hat{h}}) = \lambda(B_{\hat{h}})$ where $\lambda(S)$ denotes the measure of a set S.

Theorem 14. *Let $\hat{h}$ be the constant such that $\lambda(A_{\hat{h}}) = \lambda(B_{\hat{h}})$. Then, $\hat{h}$ minimizes $\widetilde{E(h)}$*[1].

Proof. Note that the function $\widetilde{E(h)}$ is convex in h with $h \in (a,b)$, and (a,b) a convex interval. Therefore, we are guaranteed a minimizer h^*. Now, without loss of generality, we assume that $h^* < \hat{h}$. We evaluate the cost over the two regions $A_{\hat{h}}$ and $B_{\hat{h}}$, i.e.,

$$\widetilde{E(h^*)} = \int_a^b |h_1(t) - h^*|dt = \int_{A_{\hat{h}}} |h_1(t) - h^*|dt + \int_{B_{\hat{h}}} |h_1(t) - h^*|dt. \tag{3.5}$$

We now define $B_1 = \{t : h^* < h_1(t) < \hat{h}\}$ and $B_2 = \{t : h_1(t) < h^*\}$. Note that $\lambda(A_{\hat{h}}) - \lambda(B_1) - \lambda(B_2) = 0$. We can now express $\widetilde{E(h^*)}$ in terms of $\widetilde{E(\hat{h})}$ as

$$\widetilde{E(h^*)} = \widetilde{E_{A_{\hat{h}}}}(\hat{h}) + (\hat{h} - h^*)\lambda(A_{\hat{h}}) + \widetilde{E_{B_{\hat{h}}}}(\hat{h}) - (\hat{h} - h^*)\lambda(B_2) - \alpha \tag{3.6}$$

Where $\widetilde{E_X}(\hat{h})$ denotes the cost function restricted to the subset $X \subseteq (a,b)$ and α is a positive constant that measures the difference of $\hat{h} - h^*$ on the set B_1. The maximum value of α is $(\hat{h} - h^*)\lambda(B_1)$ and hence

$$\widetilde{E(h^*)} \leq \widetilde{E_{A_{\hat{h}}}}(\hat{h}) + (\hat{h} - h^*)(\lambda(A_{\hat{h}}) - \lambda(B_1) - \lambda(B_2)) + \widetilde{E_{B_{\hat{h}}}}(\hat{h}). \tag{3.7}$$

[1] *This result also follows from a careful application of the characterization theorem of L^1 approximation. See [18] for details.*

As $\lambda(A_h) - \lambda(B_1) - \lambda(B_2) = 0$, we conclude that

$$\widetilde{E(h^*)} \leq \widetilde{E(\hat{h})} \tag{3.8}$$

and hence, $h^* = \hat{h}$. The case of $h^* > \hat{h}$ follows from symmetry. □

3.6.1 Application: Video Processing on IAMs:

We illustrate the approximation of non-parallel flow fields by parallel flow fields with the example of video resampling where we can consider a video $\mathcal{I}$ to be a curve on an IAM i.e., a video $\mathcal{I} = \{I_t, 0 \leq t \leq T\}$ with $T > 0$. This application is related to the problem of dynamic time warping (DTW) [3, 16, 30], where one is interested in measuring the similarity between two sequences that vary in time or speed. As we shall see, our application can be used for matching or aligning video sequences with a warped time axis.

Consider the IAM generated by imaging a black disk on an infinite white background starting with an initial velocity v_0 and accelerating with constant acceleration a along a fixed direction. For instance, the disk can be thought of as undergoing free fall into an infinitely deep cliff. The IAM is a one dimensional curve c and homeomorphic to $\mathbb{R}^+$, the non-negative reals. Note that the curvature is everywhere zero as $r_t = \infty$. Given an arbitrary flow field V_t along c, our goal is to analytically construct a parallel field $\tilde{V}_t$ such that $\tilde{V}_t$ is the unique parallel flow field that minimizes $\widetilde{E(h)}$. We first consider the video obtained by the action of V_t i.e. $\mathcal{I} = \{V_t(c(t))\}$. As V_t is not parallel, the video will show the disk moving in non-uniform motion. Our goal is to make the video uniform i.e.,

generate a new video $\tilde{\mathcal{I}}$ from $\tilde{V}_t$ that shows the disk moving in uniform motion.

From the physics of the problem, it is clear that $d_c(c(t), c(t+\delta_t)) = K'(v_t\delta_t + \frac{1}{2}a\delta_t^2)$ for some positive constant K' and any time increment δ_t with v_t being the velocity at time t. Now, as $\tilde{V}_t$ is to be a parallel flow field, we have that $h_{\tilde{V}}$ is a constant denoted by h. Thus, $d_c(\tilde{V}_t(c(t)), c(t)) = d_c(c(t), c(t+\delta_t)) = h$ so that $K'(v_t\delta_t + \frac{1}{2}a\delta_t^2) = h$. Rearranging this equation, we arrive at

$$\delta_t^2 + \frac{2v_t}{a}\delta_t - \frac{2h}{aK'} = 0. \tag{3.9}$$

This quadratic has real roots as the discriminant $\frac{4v_t^2}{a^2} + \frac{8h}{aK'} > 0$. Solving for δ_t, we obtain two roots $\delta_t^{1,2} = \frac{-v_t}{a} \pm \sqrt{(\frac{v_t}{a})^2 + \frac{2h}{aK'}}$ of which the (physically meaningful) positive root $\delta_t^1 = \frac{-v_t}{a} + \sqrt{(\frac{v_t}{a})^2 + \frac{2h}{aK'}} > 0$ is retained. Thus, by defining $\tilde{V}_t$ such that $\tilde{V}_t(c(t)) = c(t+\delta_t^1)$, we see that $\tilde{V}_t$ is the unique parallel flow field that minimizes $\widetilde{E(h)}$. The new video $\tilde{\mathcal{I}} = \{\tilde{V}_t(c(t))\}$ will thus show the disk moving with constant velocity. As the new video is uniform, we have effectively linearized the motion and made it independent of the acceleration of the disk. The above approach can thus be used for applications where one is interested in linearizing motion and/or alignment of video sequences [3, 30].

Chapter 4

Multiscale Structure of Parallel Flow Fields

As indicated in the previous section, the set of parallel optical fields is a very special subset of the set of all optical fields along a fixed curve c. In this section, we will construct a monoid structure (i.e., a set with an associative operation and identity) on the set of all optical fields along a *fixed* curve c and show that the class of *parallel fields* forms a submonoid of this set under some conditions on the curvature along the curve. Moreover, the monoid operation yields a multiscale structure on the set of parallel optical fields.

4.1 Monoid Structure on $\Omega(c)$

As noted previously, a clear disadvantage in dealing with the space of all optical fields along a curve is the lack of a linear, or more generally, any algebraic structure. In order to remedy this situation, we will define a binary operation on the set of optical fields that yields a monoid structure. We first fix a curve c passing through $m_1, m_2 \in M$.

Recall that a generic $V_t \in \Omega(c)$ is characterized by its motion function $h_V(t)$. Thus, operations defined on motion functions $h_V(t)$ translate to operations on $V_t \in \Omega(c)$. With this in mind, we define for $V_t, W_t \in \Omega(c)$ the sum $V_t + W_t$ to be the unique optical field

with motion function

$$h_{V+W}(t) = \min(h_V(t) + h_W(t), r_t) \tag{4.1}$$

As $h_{V+W}(t) \leq r_t$ for all t, we see that $h_{V+W}(t)$ corresponds to a unique flow field that we define to be $V_t + W_t$. This operation is clearly commutative. Note also that the trivial (parallel) field Z_t defined to be the field that acts trivially on $c(t)$, i.e.,

$$Z_t(c(t)) = c(t) \tag{4.2}$$

is characterized by the motion function $h_Z(t) = 0$ as $h_Z(t) = d_c(Z_t(c(t), c(t)) = d_c(c(t), c(t)) = 0$. Moreover, for any $V_t \in \Omega(c)$, we have that

$$Z_t + V_t = V_t. \tag{4.3}$$

We see that Z_t acts as the identity element in $\Omega(c)$. At the other extreme, there is also the unique optical field U_t characterized by

$$h_U(t) = r_t \tag{4.4}$$

that satisfies

$$V_t + U_t = U_t \tag{4.5}$$

for all $V_t \in \Omega(c)$ and hence acts as the "absorbing" element of $\Omega(c)$.

Clearly, we do not have "inverses" with respect to "+" in the sense that given a generic

$V_t \in \Omega(c)$ there does not exist a W_t such that $V_t + W_t = Z_t$. However, we do have "conjugates" with respect to "+" in the following sense. Given any $V_t \in \Omega(c)$ there is a unique $V_t^* \in \Omega(c)$ such that

$$V_t + V_t^* = U_t. \tag{4.6}$$

V_t^* is defined by its motion function

$$h_{V^*}(t) = r_t - h_V(t). \tag{4.7}$$

We refer to V_t^* as the conjugate of V_t. Moreover,

$$(V_t^*)^* = V_t. \tag{4.8}$$

Finally, we note that U_t and Z_t are conjugates.

Proposition 15. *$\Omega(c)$ is a monoid under the operation "+" defined in equation (4.1).*

Proof. We only verify associativity as Z_t provides the identity. Given $V_t, X_t, Y_t \in \Omega(c)$, we consider the sums $(V_t + X_t) + Y_t$ and $V_t + (X_t + Y_t)$. If $h_V(t), h_X(t), h_Y(t)$ are such that $h_V(t) + h_X(t) + h_Y(t) < r_t$ then both sides are clearly equal. If on the other hand, we have $h_V(t) + h_X(t) + h_Y(t) \geq r_t$ we must have that either the sum $h_V(t) + h_X(t) + h_Y(t)$ taken two factors at a time exceeds r_t or the combined sum of all three factors exceeds r_t with the sum of no two factors exceeding r_t. In the first case, we assume that $h_V(t) + h_X(t) \geq r_t$,

which implies the sum

$$(V_t + X_t) + Y_t = U_t \tag{4.9}$$

with $(X_t + Y_t) \neq U_t$,i.e.,

$$h_X(t) + h_Y(t) < r_t. \tag{4.10}$$

However, $V_t + (X_t + Y_t)$ is characterized by

$$\min(h_V(t) + \min(h_X(t) + h_Y(t), r_t), r_t) = \min(h_V(t) + h_X(t) + h_Y(t), r_t) = r_t \tag{4.11}$$

showing that

$$V_t + (X_t + Y_t) = U_t \tag{4.12}$$

as well. The other cases follow by similar arguments. □

4.2 Parallel Fields Along Curves of Constant Curvature

The addition operation defined above restricts to the set $\omega(c)$ of parallel fields along $c(t)$. However, for generic $c(t)$, the sum $V_t + W_t$ of two parallel fields $V_t, W_t \in \omega(c)$ may result in a possibly non-parallel field. For instance, if $h_V(t), h_W(t)$ are such that $h_V(t_0) + h_W(t_0) < r_{t_0}$ but $h_V(t_1) + h_W(t_1) \geq r_{t_1}$ for some t_0, t_1, then clearly, the sum is not parallel as in the first case, $h_{V+W}(t_0) = h_V(t_0) + h_W(t_0) < r_{t_0}$ while $h_{V+W}(t_1) = r_{t_1}$ so that $h_{V+W}(t)$ is not constant.

We note, however, that if r_t is constant along c, i.e., the flow radius is constant along

the path, then the above situation is vacuous. As $K_t = \frac{1}{r_t}$ is the curvature along the curve c, we are essentially requiring the optical curvature to be constant along c. We formally record the above observation:

Proposition 16. *Let c be a curve with constant optical curvature K_t. Then, the operation "+" restricted to $\omega(c)$ is a well defined operation and $\omega(c)$ is a submonoid of $\Omega(c)$.*

Proof. We need only to verify closure of "+" in $\omega(c)$ as $Z_t \in \omega(c)$. If $V_t \in \omega(c)$, then $h_V(t)$ is a constant and we will therefore suppress the argument t in $h_V(t)$. Note that as c is of constant optical curvature, r_t is a constant $r > 0$. Thus, if $V_t, W_t \in \omega(c)$, then $h_{V+W} = \min(h_V + h_W, r)$. If $h_V + h_W < r$ then as h_V and h_W are both constant so is their sum $h_V + h_W$ and

$$h_{V+W} = h_V + h_W. \tag{4.13}$$

If $h_V + h_W \geq r$, then

$$h_{V+W} = min(h_V + h_W, r) = r. \tag{4.14}$$

In either case, h_{V+W} is constant and hence,

$$V_t + W_t \in \omega(c). \tag{4.15}$$

□

Thus curves c that have constant curvature at all points, are very special: not only is parallel transport determined by a single point on the curve, but $\omega(c)$ is also a submonoid

of $\Omega(c)$.

4.3 Multiscale Structure of $\omega(c)$

In this section, we look for finite submonoids of $\omega(c)$. We would like the submonoids to be canonically defined by which we mean they depend only on the geometry of the constant curvature curve c. In particular, we construct for each positive integer k, a collection of finite submonoids $\mathcal{V}_{n,k}$ of $\omega(c)$ with n a non-negative integer and c a constant curvature path. Moreover, we will see that this collection is naturally nested, i.e.,

$$\mathcal{V}_{0,k} \subset \mathcal{V}_{1,k} \subset \cdots$$

In essence, this provides a multi-scale view of $\omega(c)$.

As $\omega(c)$ consists of parallel optical fields, we will simply denote the motion function $h_V(t)$ of $V_t \in \omega(c)$ as h_V. Moreover, we will suppress the subscript t while referring to elements of $V_t \in \omega(c)$. Also, if $V \in \omega(c)$, we mean by $\frac{V}{k}$ the element in $\omega(c)$ with motion function being the constant $\frac{h_V}{k}$. Recall also that $\omega(c)$ possesses two canonical elements $Z, U \in \omega(c) \cap \Omega(c)$ that act as the trivial and absorbing elements of $\omega(c)$ respectively.

We begin now with the construction of $\mathcal{V}_{n,k}$. Fix a positive integer k. We first set

$$\mathcal{V}_{0,k} = \{Z, U\}.$$

Next, we inductively set

$$\mathcal{V}_{n,k} = \{Z, \tfrac{U}{k^n}, \tfrac{2U}{k^n}, \ldots \tfrac{(k^n-1)U}{k^n}, U\}.$$

Now, it is clear that

$$\mathcal{V}_{0,k} \subset \mathcal{V}_{1,k} \subset \ldots.$$

Moreover, by the constant curvature condition, the sum of any two elements in $\mathcal{V}_{n,k}$ remains in $\mathcal{V}_{n,k}$ while associativity is obtained from the corresponding property in $\omega(c)$. Finally, as $Z \in \mathcal{V}_{n,k}$ for all n, k, we conclude that each $\mathcal{V}_{n,k}$ is a finite submonoid of $\omega(c)$.

We have thus obtained a sequence of finite submonoids of $\omega(c)$. Moreover, with increasing n, it is clear that an arbitrary $V \in \omega(c)$ can be uniformly approximated by $\widetilde{V} \in \mathcal{V}_{n,k}$ in the sense that $|h_V - h_{\widetilde{V}}|$ can be made arbitrarily small by choosing larger n. In other words, the sequence $\mathcal{V}_{n,k}$ is "dense" in $\omega(c)$. Finally, as the basic generators of $\mathcal{V}_{n,k}$ are $Z, U \in \omega(c) \cap \Omega(c)$, this construction is canonical in the sense that it depends only on $\{Z, U\}$, that in turn are characterized by the global geometry of the curve c.

Chapter 5

Discussion

In this thesis, we have initiated a new view of IAM theory based on the notion of transport operators where we specialized to the case of optical flow being the transport operator of choice via the key idea of *optical flow manifolds (OFMs)*. We showed that OFMs are tailor-made for image manifolds and have significantly better navigation capabilities than previous linear approaches. Our main theoretical contribution was the development of the flow metric using the ambient metric on the OFMs. Using the flow metric, we derived differential geometric analogs of tangent bundles, vector fields, parallel transport, curvature etc.

When the IAM is generated by Lie group parameters, we showed that the OFM framework includes previous algebraic methods as a special case. Moreover, since the optical neighborhood at each point is the entire IAM, we can obtain geodesics between any two images using flow operators.

A clear assumption in our analysis was that of optical flow being the transport operator of choice for IAMs. While this is true for a majority of IAMs generated by motion-induced parameter changes such as translations, rotations and unstructured plastic deformations,

there are a class of IAMs for which optical flow may not be the right transport operator. For instance, for illumination manifolds obtained by variations in the illumination of an object, optical flow may not be the transport operator we would want to use as such manifolds do not in general obey the brightness constancy requirement needed in optical flow computations. Moreover, in cases where there is significant self-occlusion during the imaging process, optical flow may not be a practical transport operator. However, by regularizing the optical flow computation to handle occlusions by removing flow operators that lead to undefined motion between pixels, one can partially circumvent this issue and the methods of this thesis can be profitably applied to this scenario as well.

A number of avenues for future work exist. First, although our development has been specific to the case of IAMs and optical flow being the corresponding transport operator, it is important to note that the basic model is extendible to a wide variety of signal ensembles with appropriately defined transport operators. For instance, a manifold model for speech signals has been proposed in [11] where appropriate transport operators and the analog of OFMs may involve a frequency domain approach. Next, once the "right" transport operator has been identified for the application in hand, one can conceivably define and study metrics similar to our flow metric and thereby develop analytic tools for further analysis.

Bibliography

[1] R. Arora and H. Parthasarathy. Optimal estimation and detection in homogeneous spaces. *IEEE Transactions on Signal Processing (TSP)*, 58(5):2623–2635, 2010.

[2] M. Belkin and P. Niyogi. Laplacian eigenmaps and spectral techniques for embedding and clustering. In *Advances in Neural Information Processing Systems 14*, pages 585–591. MIT Press, 2001.

[3] A. Bosco, A. Bruna, S. Battiato, and G. Puglisi. Digital video stabilization through curve warping techniques. *IEEE Transactions on Consumer Electronics*, 54(2):220–224, 2008.

[4] T. Brox and J. Malik. Large displacement optical flow: descriptor matching in variational motion estimation. *IEEE Trans. on Pattern Analysis and Machine Intelligence (PAMI)*, 33(3):500–513, 2011.

[5] R. R. Coifman, S. Lafon, A. B. Lee, M. Maggioni, F. Warner, and S. Zucker. Geometric diffusions as a tool for harmonic analysis and structure definition of data: Diffusion maps. In *Proceedings of the National Academy of Sciences*, volume 102, pages 7426–7431, 2005.

[6] B. J. Culpepper and B. A. Olshausen. Learning transport operators for image manifolds. In *Proc. NIPS.*, number 22, pages 423–431, 2009.

[7] M. A. Davenport, C. Hegde, M. F. Duarte, and R. G. Baraniuk. Joint manifolds for data fusion. *IEEE Transactions on Image Processing*, 19(10):2580 – 2594, 2010.

[8] M. P. do Carmo. *Riemannian Geometry*. Birkhäuser, 1992.

[9] D. L. Donoho and C. C. Grimes. Image manifolds which are isometric to euclidean space. *Journal of Mathematical Imaging and Vision*, 23:5–24, 2005.

[10] B.K.P. Horn and B.G. Schunck. Determining optical flow. *Artificial intelligence*, 17(1-3):185–203, 1981.

[11] A. Jansen and P. Niyogi. Intrinsic fourier analysis on the manifold of speech sounds. In *Proc. IEEE International Conference on Acoustics, Speech and Signal Processing (ICASSP)*, volume 1, 2006.

[12] S. H. Joshi, A. Srivastava, E. Klassen, and I. Jermyn. An efficient representation for computing geodesics between n-dimensional elastic shapes. In *Proc. IEEE Computer Vision and Pattern Recognition (CVPR)*, 2007.

[13] D. Lin, E. Grimson, and J. Fisher. Learning visual flows: a lie algebraic approach. *Proc. IEEE Conf. Computer Vision and Pattern Recognition (CVPR)*, pages 747–754, 2009.

[14] Y. Ma, S. Soatto, J. Kosecka, and S.S. Sastry. *An Invitation to 3-D Vision: From Images to Geometric Models*. Springer-Verlag, 2005.

[15] M. I. Miller and L. Younes. Group actions, homeomorphisms, and matching: a general framework. *International Journal of Computer Vision*, 41(1–2):61–84, 2001.

[16] M. E. Munich and P. Perona. Continuous dynamic time warping for translation-invariant curve alignment with applications to signature verification. In *Proc. IEEE International Conference on Computer Vision (ICCV)*, volume 1, pages 108–115, 1999.

[17] B. Nadler, S. Lafon, R. R. Coifman, and I. G. Kevrekidis. Diffusion maps, spectral clustering and reaction. 21(1):113–127, 2006.

[18] M. J. D. Powell. *Approximation Theory and Methods*. Cambridge University Press, 1981.

[19] R. P. N. Rao and D. L. Ruderman. Learning the lie groups of visual invariance. In *Neural Computation*, volume 19. MIT Press, 2007.

[20] S. Roweis and L. Saul. Nonlinear dimensionality reduction by locally linear embedding. *Science*, 290(5500):2323–2326, 2000.

[21] A. C. Sankaranarayanan, C. Hegde, S. Nagaraj, and R. G. Baraniuk. Go with the flow: Optical flow-based transport for image manifolds. In *ICCV (submitted)*, 2011.

[22] A. Srivastava, S. Joshi, W. Mio, and X. Liu. Statistical shape analysis: clustering, learning, and testing. *IEEE Trans. on Pattern Analysis and Machine Intelligence (PAMI)*, 27(4):590–602, 2005.

[23] A. Srivastava, C. Samir, S. H. Joshi, and M. Daoudi. Elastic shape models for face analysis using curvilinear coordinates. *Journal of Mathematical Imaging and Vision*, 33(2):253–265, 2009.

[24] D. Sun, S. Roth, and M.J. Black. Secrets of optical flow estimation and their principles. In *Proc. IEEE Conf. Computer Vision and Pattern Recognition (CVPR)*, June 2010.

[25] J. Tenenbaum, V.de Silva, and J. Landford. A global geometric framework for nonlinear dimensionality reduction. *Science*, 290(5500):2319–2323, 2000.

[26] A. Trouvé and L. Younes. Metamorphoses through lie group action, 2005.

[27] O. Tuzel, F. Porikli, and P. Meer. Learning on lie groups for invariant detection and tracking. *Proc. IEEE Conf. Computer Vision and Pattern Recognition (CVPR)*, pages 1–8, 2008.

[28] A. Veeraraghavan, A. K. Roy-chowdhury, and R. Chellappa. Matching shape sequences in video with applications in human movement analysis. *IEEE Trans. on Pattern Analysis and Machine Intelligence*, 27(12):1896–1909, 2005.

[29] M.B. Wakin, D.L. Donoho, H. Choi, and R.G. Baraniuk. The multiscale structure of non-differentiable image manifolds. In *Proc. SPIE Wavelets XI*, 2005.

[30] K. Wang and T. Gasser. Alignment of curves by dynamic time warping. *Annals of Statistics*, 25(3):1251–1276, 1997.

[31] L. Younes. Computable elastic distances between shapes. *SIAM J. of Applied Math*, 58(2):565–586, 1998.